International Journal of Pharmacy and Pharmaceutical Sciences

ISSN- 0975-1491 Vol 8, Issue 1, 2016

Original Article

GREEN SYNTHESIS OF SILVER NANORODS USING AQUEOUS EXTRACT OF *KALANCHOE PINNATA* FRESH LEAVES AND ITS SYNERGISTIC EFFECT WITH CIPROFLOXACIN AND ANTIBIOFILM ACTIVITIES

ROHAN SHARADANAND PHATAK[1], ANUP HENDRE[2]

[1]Directorate of Research, [2]Department of Biochemistry, Krishna Institute of Medical Sciences Deemed University, Karad, Maharashtra India
Email: phatak.rohan1983@gmail.com

Received: 18 Aug 2015 Revised and Accepted: 18 Nov 2015

ABSTRACT

Objective: The present study was aimed to investigate antibacterial and antibiofilm activities of AgNPs alone and its combination with ciprofloxacin against various human pathogenic bacteria strains.

Methods: Reproducible, energy efficient, eco-friendly green synthesis of silver nanoparticles (AgNPs) using aqueous extract of *Kalanchoe pinnata* fresh leaves based on photoirradiation was carried out. These photosynthesized AgNPs were characterized by infrared spectroscopy, scanning electron microscopy with energy dispersive X-ray spectroscopy, transmission electron microscopy, zeta potential, differential scanning calorimetry, differential thermal analysis and particle size analysis.

Results: From the results, AgNPs showed the desired physicochemical properties in terms of optical, structural, thermal and photocatalytic properties. Also, it is observed that Gram-negative bacteria strains are more vulnerable to both AgNPs as well as conjugating ciprofloxacin with AgNPs rather than Gram-positive bacteria strains.

Conclusion: Enhanced antibacterial effect was observed in the conjugation of ciprofloxacin with AgNPs rather than antibiotic or AgNPs alone. AgNPs showed an excellent inhibitory effect in the formation of biofilm.

Keywords: Green synthesis, *Kalanchoe pinnata*, AgNPs, Antibacterial, Antibiofilm.

INTRODUCTION

Today's age, increasing antibiotic resistance is undeniable consequences for emerging Multi-Drug Resistant (MDR) strains of bacteria throughout the world and biofilm formation in the biomaterials has become a major concern in the biomedical fields especially for implants and medical devices in the hospital. According to the current clinical reports, it has been estimated the incidence of nosocomial infections in patients admitted in the Intensive Care Unit (ICU) has more than patients admitted in general hospital [1]. Nosocomial infections are frequently associated with biofilm which leads to a huge burden to the health care system which costs in the budget up to billions of dollars [2]. In the medical and healthcare systems, biomaterials have emerged as a fundamental element which holds an outstanding position of the biomedical fields. Biomaterial-Associated Infections (BAI) is the rate of occurrence of bacterial infections associated with the use of biomaterials [3]. Bacteria which are involving in BAI are resistant to antibiotics and host immune system. BAI is becoming a serious problem in the healthcare system and have turned out to the main factor for leading microbial infection risks. Failure of implanting biomaterial is the one of a major contributing factor of BAI, and infectivity with microorganisms during the process of surgery, hospitalization causing the onset of BAI [4]. Thus, the chemical modification of the biomaterial surface may prevent to microbial biofilm formation. Silver is well known for its antimicrobial properties since many decades, silver and silver-containing compounds have used as antimicrobial agents for treating bacterial infections [5]. Therefore, silver nanoparticles (AgNPs) have become an attracting interest in nanotechnologists recently than those uses of bulk silver-containing compounds due to its unique properties like a cost effective, feasible, large surface area and its vast scope in the biomedical applications [6]. For that, AgNPs can fabricate with such biomaterials by applying on the surface of biomaterials as a coating agent.

Conventional physical and chemical routes of synthesizing nanoparticles have many disadvantages such as poor yield, time-consuming procedure, high expensive, hazardous to use, and required high energy to induce the chemical reaction. Also these methods are involved in the use of toxic reducing agents which affects on the environment. So there is a need of the hour to develop natural, high yield, cost-effective, nontoxic, time saving, eco-friendly procedure and cheap availability of raw material. For that biological approach is the most applicable for environmentally sound and suitable to use as an alternative method to these conventional physical and chemical methods [7]. In this study sunlight irradiation was used to extend the phyto-synthesis of AgNPs using *Kalanchoe pinnata* fresh leaves (FLKP). Sunlight radiation accelerates the reduction of silver nitrate solution to AgNPs within a short period of time. Photo-irradiation based biosynthesis strategies provide safer process and narrow size distribution [8]. In our previous studies, aqueous extract of sun-dried leaves of this plant has been utilized to initiate AgNPs with the assistance of sunlight irradiation and its photocatalytic activities [9]. The present study was aimed to investigate antibacterial and antibiofilm activities of AgNPs alone and its combination with ciprofloxacin against various human pathogenic bacteria strains.

MATERIALS AND METHODS

Green synthesis of silver nanoparticles by aqueous extract of *Kalanchoe pinnata* leaves [9]

Fresh leaves of *Kalanchoe pinnata* were boiled in an adequate volume of distilled water for 15 min at 60°C to maximize the extraction. This aqueous extract was filtered through Whatman filter paper. 5 ml of aqueous extract of *Kalanchoe pinnata* leaves was added to 0.1M silver nitrate solution and stirring the reaction mixture well. The reaction mixture was exposed to sunlight for a few minutes, and a change in color was observed. Biogenic AgNPs were centrifuged to remove any excess of extract and unreduced silver ions solution and stored in a suitable container (FLKP).

Physicochemical characterization

Fourier Transform Infra Red (FTIR) spectroscopy analysis of the dried AgNPs was carried out through using Nicklet 380 Thermo, US

Fourier Transform Infrared Spectrometer. Morphology of phytosynthesized AgNPs was screened under Scanning Electron Microscopy-Energy Dispersive X-ray (SEM-EDX) spectroscopy and Transmission Electron Microscopy (TEM). Electrophoretic movement of charged AgNPs was determined by Electrophoretic Light Scattering (ELS) under an applied electric field from the Doppler shift of scattered light for zeta potential determination (Delsa Nano, Beckman Coulter). Differential Scanning Calorimetry (DSC) is a thermoanalytical technique in which the difference in the amount of heat required to increase the temperature of a sample and reference is measured as a function of temperature (SIIO 6300 with Autosampler, Japan). Thermogravimetric analysis (TGA-DTA) spectra have been recorded in the range from room temperature to higher temperature using the simultaneous thermal system. A ceramic (Al_2O_3) crucible was used for heating and measurements were carried out in the suitable condition at the heating rate of 10 °C/min. The particle size of photosynthesized AgNPs was determined by ELS under an applied electric field from the Doppler shift of scattered light for zeta potential determination (Delsa Nano, Beckman Coulter).

Antibacterial activity of silver nanoparticles

AgNPs synthesized using an aqueous extract of *Kalanchoe pinnata* fresh leaves was tested for antimicrobial activity by agar well diffusion method against different pathogenic microorganisms *Staphylococcus aureus*, *Pseudomonas aeruginosa*, *Salmonella typhi*, *Streptococcus pyogens*. The pure cultures of bacteria were sub-cultured on Mueller Hinton Agar. Each strain was swabbed uniformly onto the individual plates using sterile cotton swabs. Wells of 8 mm diameter were made on nutrient agar plates using sterile micropipette tips. Using a micropipette, 20µl of nanoparticles solution was poured onto each well on all plates. After incubation at 37°C for 24 h, the diameter of zone inhibition was measured in millimeter, and was recorded as mean±SD.

Bioassay of antimicrobial activities

Test microorganisms

The antimicrobial activity of phytosynthesized AgNPs was tested against four pathogenic microbial strains, varying between 3 gram-positive and 3-gram negative bacteria species.

Agar well diffusion method

The antimicrobial activity of phytosynthesized AgNPs was tested by standard agar well diffusion method as described in CLI guidelines [10]. All the experiments were carried out in duplicates. It was used to measure the efficacy of AgNPs in terms of zone inhibition against clinical isolates of Gram-positive and Gram negative bacteria strains available from Krishna hospital, Karad.

Conjugating antibiotic with silver nanoparticles

The antimicrobial activity was checked with the standard antibiotic discs, AgNPs extract and Ciplox antibiotic discs conjugated with 100 µl of AgNPs against bacterial strains. Prior to incubation for 24 h at 37◦C, inhibition zones were measured in mm. Antibacterial activity has been increased manifold times in conjugation of antibiotic with AgNPs rather than individual either of antibiotic or silver nanoparticles.

Antibiofilm effect of phytosynthesized silver nanoparticles

Biofilm formation assay and biofilm inhibition assay were performed in accordance to method [11].

Biofilm formation assay

Biofilm formation assay was performed in eppendorf centrifuge tubes. The bacterial suspension was adjusted to be equivalent to 0.5 McFarland's standard. A serial dilution of bacterial suspension was made from 108cfu/ml till 10cfu/ml. Eppendorf centrifuge tubes were filled with 1 ml of bacterial suspension and was incubated for 24 h at 37 °C. After incubation, the bacterial suspension in the eppendorf centrifuge tubes was gently removed. The wells were washed with phosphate buffer saline (PBS pH 7.2) to remove free-floating 'planktonic' bacteria. Biofilm of bacteria strains adhered to the wall of eppendorf centrifuge tubes were stained with crystal violet (0.1%, w/v). Excess stain was rinsed off by washing with deionized water, and 1 ml of 95% ethanol was added to these tubes which dissolves the stained biofilm and transferred to the test tubes respectively. To these test tubes, 2 ml of 95% ethanol was added to adjust in the volume of the cuvette when taking optical densities (OD) of stained adherent bacteria were determined against 590 nm. The optical density value was considered as the formation of biofilm on the surface of the tubes. The experiment was performed in triplicates.

Biofilm inhibition assay

Biofilm inhibition assay was performed in eppendorf centrifuge tubes. Eppendorf centrifuge tubes were filled with 1 ml of bacterial broth media. AgNPs solution was diluted two-fold from 20µl to 1.25µl in the bacterial suspension. The bacterial suspension was adjusted to be equivalent to 0.5 McFarland's standard. A volume of 100µl of bacterial suspensions were transferred to these serially diluted AgNPs suspended in the bacterial broth media. These were incubated for 24 h at 37 °C. After incubation, the bacterial suspension of eppendorf centrifuge tubes was gently removed. The wells were washed with phosphate buffer saline (PBS pH7.2) to remove free-floating 'planktonic' bacteria. Biofilm of bacteria strains adhered to the wall of eppendorf centrifuge tubes were stained with crystal violet (0.1%, w/v). Excess stain was rinsed off by washing with deionized water, and 1 ml of 95% ethanol was added to these tubes which dissolve the stained biofilm and transferred to the test tubes respectively. To these test tubes, 2 ml of 95% ethanol was added to adjust in the volume of the cuvette when taking optical densities (OD) of stained adherent bacteria were determined against 590 nm. The optical density value was considered as the formation of biofilm on the surface of the tubes. The experiment was performed in triplicates.

RESULTS

FTIR

In fig. 1, FTIR spectrum of phytosynthesized AgNPs showed the two strong IR bands of hydroxyl and phenols (3453.06 cm^{-1}), whereas C=C stretch of benzene and amide-I linkage (1637.76 cm^{-1}) and other IR bands of (2076.95 cm^{-1}) and (559.46 cm^{-1}). The broadband appearing at (3453.06 cm^{-1}and3452.81 cm^{-1}) are assigned for O–H stretching vibration indicating the presence of hydroxyl and phenolic hydroxyl groups, responsible as the reducing as well as capping agents. Absorption peak (1631.39 cm^{-1} and 1631.27 cm^{-1}) in the infrared region of the electromagnetic spectrum exhibits the binding of amide linkage with AgNPs which may be assigned to the carbonyl stretch in proteins and clearly indicates the presence of protein as a capping agent for AgNPs. FTIR spectrum of AgNPs in this study is found to be identical with FTIR spectrum of AgNPs in our previous study [9]. No any difference found in between FTIR spectra of both AgNPs biosynthesized by sundried and fresh leaves of *Kalanchoe pinnata* respectively.

SEM-EDX

Each of the colloidal solution containing AgNPs was centrifuged at 4,000 rpm for 15 min and the pellets were discarded and the supernatants were again centrifuged at 5,000 rpm for 30 min. Supernatants were discarded, and the final pellets were dissolved in 0.1 ml of deionized water. The pellet was carefully placed on a glass coverslip followed by air-drying. The coverslip itself was screened under SEM analysis. AgNPs as polycrystalline structure were revealed by SEM-EDX as shown in fig. 2.

TEM

Morphology of AgNPs was investigated by TEM in fig. 3. TEM images have shown AgNPs about below 10 nm average diameter and spherical rod shape.

Zeta potential

Zeta potential of AgNPs was found to be-27.3mV in fig. 4. A negative value in the zeta potential of AgNPs might be possible due to the presence of hydroxyl (OH^-) functional groups gets adsorbed on the surface of AgNPs during capping which are responsible for

increasing stability owing to electrostatic repulsion between each nanoparticle. The abovementioned FTIR spectrum has shown broadband of hydroxyl functional group (3441.32 cm^{-1}) which confirms the presence of hydroxyl groups on the surface of AgNPs.

DSC

The well pointed DSC curves of AgNPs are shown in Fig.5. AgNPs showed a sharp endothermic peak at 108.59 °C due to transition temperature (Tg). The denaturation enthalpy of both of AgNPs is closer to single stage decomposition. Earliest weight loss for AgNPs took place at above 100 °C. Therefore, the denaturation temperature displayed in the DSC curves for AgNPs suggests that the phytochemicals present in the extract which are responsible for the reduction of Ag+to Ag ° (nanoparticle) could be a highly thermal stable compound.

TGA-DTA

TGA and DTA curves of AgNPs are shown in Fig.6. It is observed from TGA-DTA curve of AgNPs that weight loss of the sample occurred in the temperature region between 80-90 °C displayed in fig. 6.

Particle size analysis

The particle size determination of phytosynthesized AgNPs was shown based on intensity. Particle size analysis chart showed in fig. 7. The mean particle size (z-average), polydispersity index (PI) of phytosynthesized AgNPs was determined.

Antibacterial activity of AgNPs

Bacteria susceptibility test of AgNPs was observed in the inhibition zone size (mm) in fig. 8 and susceptibility rate are following here: *Pseudomonas aeruginosa>Salmonella typhi>Streptococcus pyogens> Staphylococcus aureus*.

In table 1, "increase in fold area" was measured to differentiate the potency between antibiotic conjugated with AgNPs and antibiotic alone. It was observed in ascending order as: *Salmonella typhi>Staphylococcus aureus>Streptococcus pyogens>Pseudomonas aeruginosa*

Antibiofilm effect of phytosynthesized AgNPs

Biofilm formation was monitored *in vitro* by investigating the binding ability of bacterial cells to 0.1% crystal violet adhered to eppendorf tube. The optical density value was used as an indicator for the ability to form biofilm in bacteria strains as shown in fig. 9.

Antibiofilm capacity of phytosynthesized AgNPs was screened to inhibit biofilm of four pathogenic bacteria strains adherence to eppendorf tube as shown in fig. 10.

Table 1: Zone inhibition of phytosynthesized AgNPs

Test samples	*S. aureus*	*S. pyogenes*	*S. typhi*	*P. aeruginosa*
AgNPs(20µl/ml) (mm)	11	10	11	19
Ciplox(5mcg) (mm) [A]	13	15	24	36
Ciplox(5mcg)+AgNPs (mm) [B]	15	16	30	38
Increase in fold area	0.331	0.137	0.562	0.114

Ciplox-Ciprofloxacin, Mean surface area of the inhibition zone was calculated for each from diameter, Increase in fold area was calculated as (B2-A2)/A2, where A and B are the inhibition zones for Ciplox and Ciplox+AgNPs respectively.

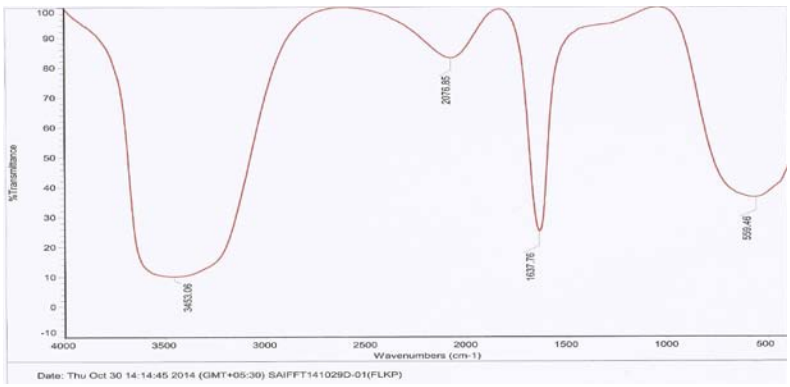

Fig 1: FTIR spectra of phytosynthesized AgNPs

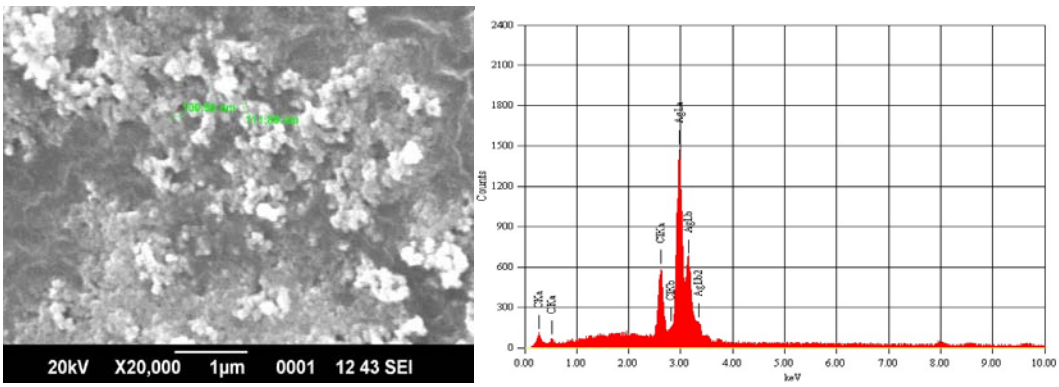

Fig. 2: SEM-EDX image of phytosynthesized AgNPs

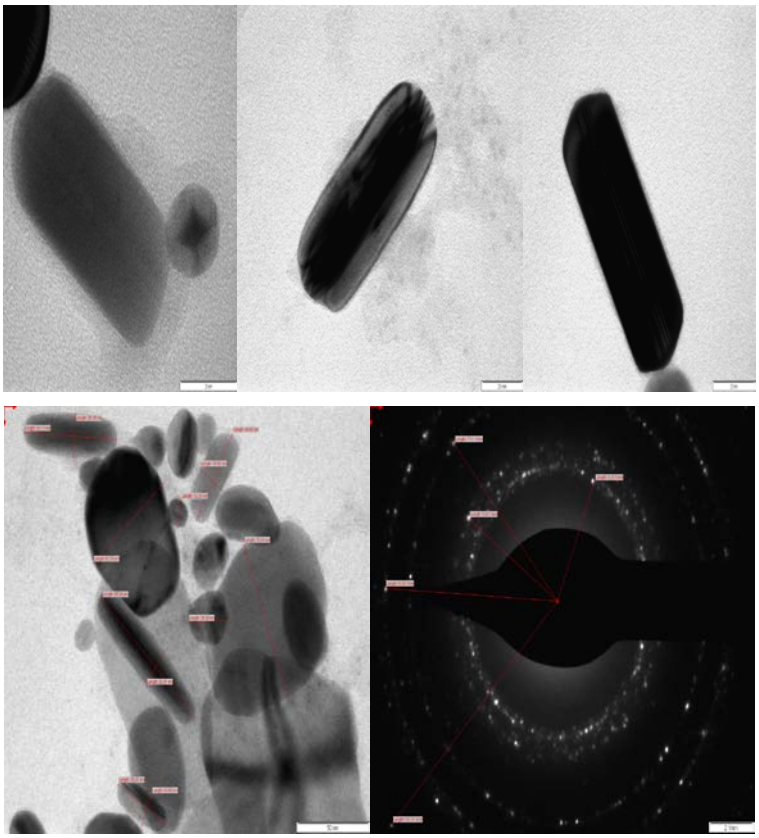

Fig. 3: TEM different dimensional images of phytosynthesized AgNPs

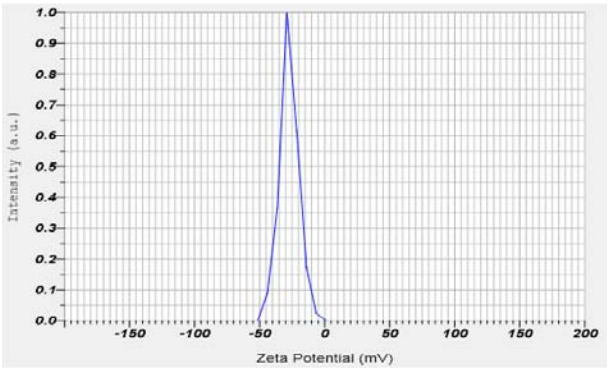

Fig. 4: Zeta potential of phytosynthesized AgNPs

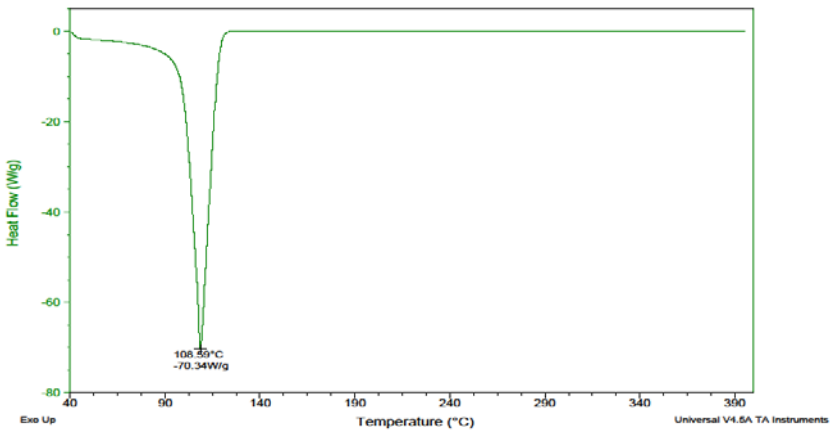

Fig. 5: DSC spectra of phytosynthesized AgNPs

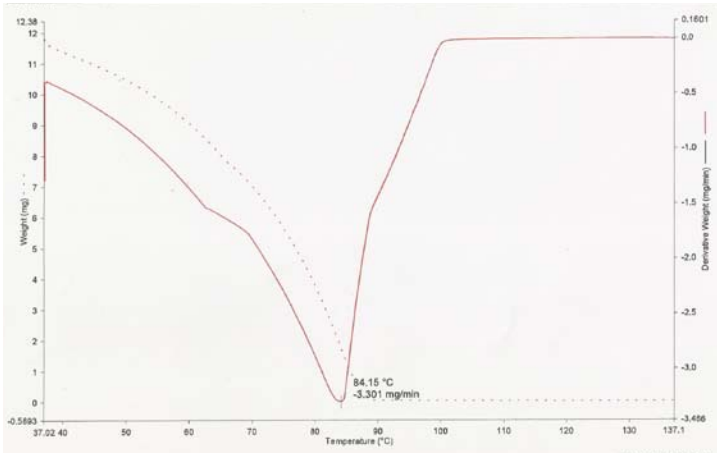

Fig. 6: TGA-DTA spectra of phytosynthesized AgNPs

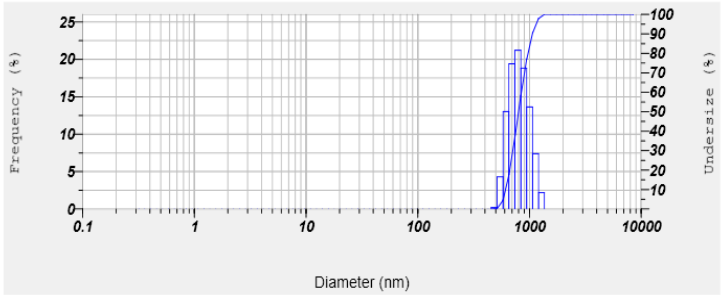

Calculation Results

Peak No.	S.P.Area Ratio	Mean	S. D.	Mode
1	1.00	822.2 nm	171.9 nm	786.2 nm
2	---	--- nm	--- nm	--- nm
3	---	--- nm	--- nm	--- nm
Total	1.00	822.2 nm	171.9 nm	786.2 nm

Cumulant Operations

Z-Average : 522.5 nm
PI : 2.342

Fig. 7: Particle size analysis of phytosynthesized AgNPs

Streptococcus pyogens

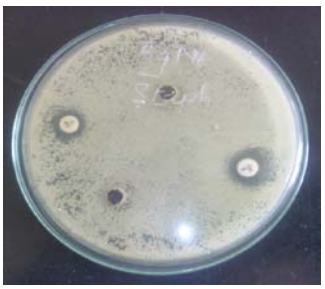

Staphylococcus aureus

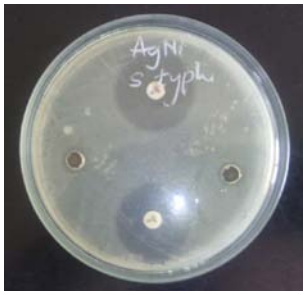

Salmonella typhi

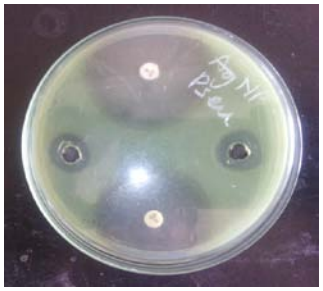

Pseudomonas aeruginosa

Fig. 8: Synergistic activity of AgNPs with ciprofloxacin against gram positive and gram negative bacterial strains

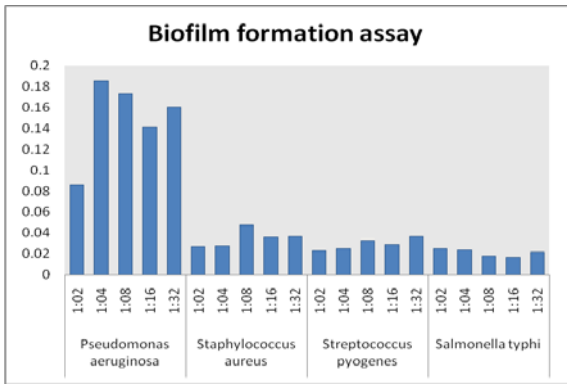

Fig. 9: Biofilm formation assay of phytosynthesized AgNPs

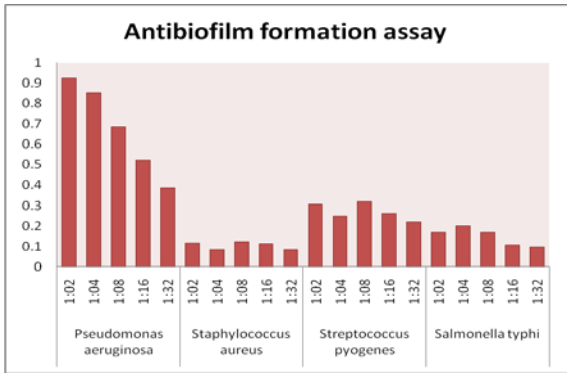

Fig. 10: Antibiofilm formation assay of phytosynthesized AgNPs

DISCUSSION

Antibacterial activities of AgNPs; its synergistic effect with ciprofloxacin and antibiofilm effect of AgNPs

From the results, it is observed that Gram-negative bacteria strains are more vulnerable to both AgNPs as well as conjugating ciprofloxacin with AgNPs rather than Gram-positive bacteria strains. In our previous study, antibacterial activities of AgNPs biosynthesized by latex of *S. grantii* were confirmed [12].

An enhanced antibacterial activity was found in the case of ciprofloxacin conjugated AgNPs rather than individual either of antibiotic or silver nanoparticles alone. The cell wall of Gram-negative bacteria consists of peptidoglycan layer and Lipopolysaccharide (LPS) as outer membrane whilst the cell wall in Gram-positive bacteria is composed of a thick layer of peptidoglycan consisting of linear polysaccharide chains cross-linked with peptides forming a rigidly structured cell wall [13]. Thus, this rigid cross-linking of cell wall minimizes the accessibility of AgNPs to penetrate whereas AgNPs may enter through the porin channel present in the cell wall of Gram-negative bacteria. AgNPs conjugated ciprofloxacin destroyed the LPS outer membrane of Gram-negative by binding with peptidoglycan permitting to penetrate. Synergism may be possible due to bonding between antibiotic and AgNPs as there is some active functional groups like hydroxyl group which chelates with AgNPs [13]. Many studies have been reported that synergistic effect was observed for inhibiting bacterial growth when any conventional antibiotic combined with AgNPs [13, 14]. Combinational studies of AgNPs with antibiotic are warranted in the further investigation [6].

Ciprofloxacin is second-generation of quinolone antibiotic having a broad spectrum against Gram-positive and Gram negative bacteria. Its mechanism of action is based on inhibition of DNA gyrase, topoisomerase II, topoisomerase IV, and other enzymes required separating bacterial DNA in turn to block cell division [15]. Here in the present study, ciprofloxacin plus AgNPs have shown many inhibitory effects against both types of bacteria. It may propose that AgNPs have a naturally higher affinity towards sulfur containing proteins like thiol group and phosphorous containing proteins like DNA in the bacterial cells. These are most likely binding sites available for AgNPs. AgNPs could damage bacterial cells through binding phosphate group of bacterial DNA due to altering protein structure [3]. By interacting with thiol, functional group of enzymes AgNPs inactivate the transcription and translating enzymes. AgNPs also arrest the bacterial growth by modulating phosphotyrosine of the bacterial proteins [14]. In combination with ciprofloxacin AgNPs, it could exert synergistically deleterious effect on the bacteria by damaging bacterial DNA and inactivating vital enzymes. Several mechanisms have been explained on the antibacterial activities of metallic nanoparticles. Electrostatic interactions between AgNPs and bacterial cell membranes lead to leakage of the cell. Hydrogen peroxide, superoxide radicals, hydroxyl radicals and singlet oxygen including ROS responsible for inducing oxidative stress to the bacterial cells which cause damage the protein and DNA in bacteria [3].

A biofilm is a bacterial population inhabited within the self-created exopolysaccharide matrix [11]. Free floating bacteria prevail in an aqueous medium which are main causes for biofilm formation, so it is called as planktonic microorganisms. It begins to form the biofilm when planktonic bacteria bind irreversibly on any surfaces. Then it forms extracellular polymer matrix [11] through thin layered condensations of microbes attaching on the surface structure. Planktonic bacteria are often to get adsorb on the surface where the source of organic nutrients like electrolytes, water, and organic substances are accessible, and further remain attached lastingly to the site [11]. Polysaccharide intercellular adhesin and accumulation-associated protein are the main contributing factors to form biofilm [16]. Biofilm minimizes the diffusion of substances; binding of antimicrobial agents; restrict the doorway of proteins which are having larger molecular weight with antimicrobial properties, enzymes, and complement [17]. It produces certain advantages by providing such hostile environmental situation where bacteria are allowed to strive; by protecting them from adverse conditions of change in humidity, pH, and concentration of nutrients [11]. They have more antimicrobial resistance due to its inherent architecture. This biofilm restricts dispersion and penetration of antimicrobial agents in turn to reducing the efficiency of antibiotics. Thus, the alternative antimicrobial strategies are essential to combat multidrug-resistant infections [5]. Although the penetration rate of AgNPs into biofilm may vary depending upon uptake of AgNPs by bacterial cells. Inhibition effect of AgNPs may also hinder with the increase in the bacterial cell number may due to agglomeration of AgNPs [11]. Sessile bacteria are restricted mobile; have grown as colonies protected in exopolysaccharide matrix on the surface containing a limited supply of nutrients, so they are resistant to the effects of antibiotics and environmental factors while planktonic bacteria are motile, unprotected and susceptible [2].

The present study is also the same line with the study by Gudikandula *et al.* [18].

CONCLUSION

From remarkable results in the present study, it is learnt that silver nanoparticles can photosynthesized by use of plant extract alternative to physical and chemical synthesis; can formulate into antibacterial nanoparticles by conjugating with antibiotic as a means of overcoming the problem of drug resistance in human pathogenic bacteria and can fabricate nanoparticles coated onto the surface of biomaterials as antibiofilm protective coating to prevent biofilm formation.

ACKNOWLEDGEMENT

Authors are acknowledged to Diyalabs Mumbai, SAIF Kochi and SAIF-IIT Bombay for their exemplary analytical services. Authors express their gratitude to Head of Department and technicians in Department of Microbiology, Krishna Institute of Medical Sciences, Karad.

CONFLICT OF INTEREST

Authors declare that there is no conflict of interest.

REFERENCES

1. Dasgupta S, Das S, Chawan NS, Hazra A. Nosocomial infections in the intensive care unit: Incidence, risk factors, outcome and associated pathogens in a public tertiary teaching hospital of Eastern India. Indian J Crit Care Med 2015;19:14-20.
2. Olson ME, Ceri H, Morck DW, Buret AG, Read RR. Biofilm bacteria: formation and comparative susceptibility to antibiotics. Can J Vet Res 2002;66:86-92.
3. Sathyanarayanan MB1, Balachandranath R, Genji Srinivasulu Y, Kannaiyan SK, Subbiahdoss G. The effect of gold and iron-oxide nanoparticles on biofilm-forming pathogens. ISRN Microbiol 2013:272086. doi: 10.1155/2013/272086. [Article in Press]
4. Drancourt M, Stein A, Argenson JN, Roiron R, Groulier P, Raoult D. Oral treatment of Staphylococcus spp. infected orthopedic implants with fusidic acid or ofloxacin in combination with rifampicin. J Antimicrob Chemother 1997;39:235-40.
5. Habash MB, Park AJ, Vis EC, Harris. The synergy of silver nanoparticles and aztreonam against Pseudomonas aeruginosa PAO1 biofilms. Antimicrob Agents Chemother 2014;58:5818-30.
6. Gurunathan S, Han JW, Kwon DN, Kim JH. Enhanced antibacterial and antibiofilm activities of silver nanoparticles against gram-negative and gram-positive bacteria. Nanoscale Res Lett 2014;9:373.
7. Padalia H, Moteriya P, Chanda S. Green synthesis of silver nanoparticles from marigold flower and its synergistic antimicrobial potential. Arabian J Chem 2014;8:732-41.
8. Ullah N, Li D, *et al.* Photo–irradiation based biosynthesis of silver nanoparticles by using an evergreen shrub and its antibacterial study. Digest J Nanomater Biostructures 2015;10:95-105.
9. Phatak RS, Hendre AS. Sunlight-induced green synthesis of silver nanoparticles using sun-dried leaves extract of Kalanchoe pinnata and evaluation of its photocatalytic potential. Pharm Lett 2015;7:313-24.
10. Clinical and Laboratory Standards Institute. Wayne, PA, 1995: 15th informational supplement. Document M100-S15; 2000.
11. Palanisamy NK, Ferina N, Amirulhusni AN, Mohd-Zain Z, Hussaini J, Ping LJ, *et al*. Antibiofilm properties of chemically synthesized silver nanoparticles found against *Pseudomonas aeruginosa*. J Nanobiotechnol 2014;12:2.
12. Durgawale PP, Phatak RS, Hendre AS. Biosynthesis of silver nanoparticles using latex of Syandenium grantii hook f and its assessment of antibacterial activities. Dig J Nanomater Biostructures 2015;10:846-53.
13. Balaji RR, Singh P. Synergistic effect of silver nanoparticles with the cephalexin antibiotic against the test strains. Bioresearch Bull 2013;2:4.
14. Naheed Ahmad, Seema Sharma, Singh VN, Shamsi SF, Fatma A, Mehta BR. Biosynthesis of silver nanoparticles from *Desmodium triflorum*: A novel approach towards weed utilization. Biotechnol Res Int 2011. http://dx.doi.org/ 10.4061/2011/454090. [Article in Press]
15. Drlica K, Zhao X. DNA gyrase, topoisomerase IV, and the 4-quinolones. Microbiol Mol Biol Rev 1997;61:377-92.
16. Zaat SAJ, Broekhuizen CAN, Riool M. Host tissue as a niche for biomaterial-associated infection. Future Microbiol 2010;5:1149-51.
17. Ansari MA, Khan HM, Khan AA. Antibiofilm efficacy of silver nanoparticles against biofilm of extended spectrum b-lactamase isolates of *Escherichia coli* and *Klebsiella pneumoniae*. Appl Nanosci 2013;4:859-68.
18. Gudikandula K, Sriyamjalla SK, V Pranitha, Alha M, Charaya S. Biogenic synthesis of silver nanoparticles and their synergistic effect with antibiotics: a study against Salmonella sp. Int J Pharm Pharm Sci 2015;7:84-8.